Research Article

Journal of Environmental Nanotechnology

NiO at Paraffin Wax Soot Carbon Nanocomposites for Congo Red Dye Removal from Waste Water

I. Muralisankar[1*], S. Agilan[2], T. Venkatachalam[2], E.P. Subramaniam[1], P. Thanapackiam[1]
[1]Department of Chemistry, Coimbatore Institute of Technology, Coimbatore, TN, India
[2]Department of Physics, Coimbatore Institute of Technology, Coimbatore, TN, India
Received: 08.11.2018 Accepted: 22.12.2018 Published: 30-03-2019
*imuralikavitha@gmail.com

ABSTRACT

In this work, Nickel oxide-activated carbon nanocomposites (NiO-CNC) were synthesized using the carbon soot of paraffin wax by a simple combustion method and tested as an adsorbent for the removal of hazardous Congo red dye (CR) in the aqueous phase. The adsorption studies have been carried out thoroughly and elucidated with the impact of important parameters, *viz*, pH of the dye solution, initial dye concentration, contact time and sorbent dose, which were found to be 11, 200 ppm, 60 min, and 0.035 g/L, respectively. Sorption kinetics and isotherm modeling were studied and checked for their applicability with dye sorption system using synthesized NiO-CNC by non-linear fit. The co-relation coefficient of the Langmuir and Redlich-Peterson isotherm model was found to be 0.99 > 1. The pseudo-second order kinetic model was fitting well with the obtained equilibrium data with maximum sorption capacity (q_e= 401.35 mg/g). The thermodynamic parameters have indicated that NiO-CNC system was more feasible, exothermic and spontaneous.

Keywords: Carbon nanocomposite; Nickel oxide; Non-linear fit; Sorption kinetics; Thermodynamic studies.

1. INTRODUCTION

Synthetic dyes are found in toxic effluents from the textile, metal finishing, leather, plastics and paper industries, which damage water bodies and its environment. There are several phases of processing, dyeing and product finishing; all these sectors need a lot of water. Synthetic dyes are very poisonous and visible in these businesses, and even a little amount of colour can poison the entire water system. As a result, removing these colours from polluted water before they enter the environment has become a top priority (Gong *et al.* 2009; Shahryari-Ghoshekandi and Sadegh, 2014; Wang *et al.* 2008).

Owing to the fact that synthetic dyes cause considerable damage to the flora and fauna of the ecosystem, several methods *viz*, precipitation, coagulation, reverse osmosis, ion-exchange and adsorption are adopted, but they fail to meet the requirements in two aspects - cost-effectiveness and recycling nature (Marti *et al.* 2008; Liang *et al.* 2009; Gupta *et al.* 2015; Zare *et al.* 2015). Nevertheless, adsorption is found to be the most efficient and cost-effective method in the removal of trace amounts of dyes in the aqueous media (Sadegh *et al.* 2015a; 2015b; Gupta *et al.* 2015). Mesoporous materials like activated carbon, zeolites, biomaterials, nanoparticles and polymers, are some adsorbents extensively used for adsorption of toxic dyes (Gupta *et al.* 2015; Zare *et al.* 2015; Sadegh *et al.* 2015a; 2015b; Gupta *et al.* 2015). Carbon nanotubes (Mahmoodian *et al.* 2014; Gupta *et al.* 2011; 2013a; 2013b; Nekouei *et al.* 2015; Ghaedi *et al.* 2015) and chemically modified polymers (Vidhyadevi *et al.* 2013; Murugesan *et al.* 2012; Kirupha *et al.* 2015), have attracted greater attention as adsorbents for the removal of dyes and metals because of their high adsorption capacity. Carbon nanotubes are unique in their structure and possess many outstanding mechanical, electronic and optical properties (Roberts *et al.* 1977), but the adsorption capacity is considerably low. Researchers try to find out a better solution for the synthesis of CNTs with good adsorption capacity. SWCNTs and MWCNTs were prepared using different techniques such as evaporation, laser ablation, chemical vapor deposition, electrolysis and flame synthesis (Iijima, 1991; Das *et al.* 2014; Iijima and Ichihashi, 1993; Terrones, 2003; Farhat and Scott, 2006; Rafique and Iqbal, 2011). Some inorganic metals and organo-metallic complexes are used as catalysts in this method. The catalysts are generally made from metals or their salts (Nyamori *et al.* 2008). Pyrolysis is the most economical, cost-effective methodology in synthesizing CNTs with source materials, which includes methane, acetylene, ethanol, benzene and polyvinyl alcohol (PVA) (Dikio *et al.* 2010; Dikio and Bixa, 2011; Benito *et al.* 2009; Liu *et al.* 2003; Shao *et al.* 2000; Jin *et al.* 2007).

Focus has been laid in the present study upon the simple synthesis of nickel oxide-impregnated carbon composite (NiO-CNC), synthesized by burning paraffin wax along with nickel acetate by controlled pyrolysis methodology and its use as an adsorbent for the removal of Congo red (CR) anionic dye, in an aqueous medium.

The effect of experimental parameters which influence the sorption process, such as contact time (t), solution pH of the dye solution, initial dye concentration, adsorbent dose and temperature (T) have been investigated. Adsorption isotherms and kinetics were applied to different isotherm models to find out the best fit model which describes the sorption process and the mechanism involved with the obtained experimental data. The thermodynamic parameters such as enthalpy change (ΔH°), Gibbs free energy (ΔG°) and entropy change (ΔS°) were calculated.

2. MATERIALS AND METHODS

Nickel acetate (Ni $(CH_3CO_2)_2$) (Sigma-Aldrich), Paraffin wax (Merck), Congo red (Labchem) were used as such without purification for synthesis and adsorption study. All working solutions for adsorption studies were prepared using de-ionized water with an error deviation of less than ±1%.

2.1 Analytical Methods

The X-ray diffraction patterns of NiO-CNC, were recorded using a Bruker AXS D8 Advance diffractometer with Cu-Ka radiation. The surface morphology, composition and particle size were analyzed using a Leo Gemini 1530 Scanning Electron Microscope (SEM) at an accelerating voltage of 15 kV with Energy-dispersive studies (EDS) and Transmission electron microscopy (TEM, JEOL model JEM 2011) at an accelerating voltage of 200 kV. Raman spectra of NiO-CNC were recorded using the Renishaw in the micro-Raman spectrometer, using an argon laser excitation wavelength of 514 nm at 20 mW powers with an illumination spot of size 1 μm and an acquisition time of 90 s. The concentration of the dye solution before and after adsorption experiments were measured using a UV-Visible spectro-photometer (Shimadzu, Japan).

2.2 Synthesis of Nickel Oxide Activated Carbon Nanocomposite (NiO-CNC)

The mixture of precursors 35.7 g of nickel acetate ($Ni(CH_3CO_2)_2$) (Sigma-Aldrich) and 36.7 g paraffin wax (Merck) (fused) were ground well in an agate mortar and taken in a China dish (4 inch in diameter). The mixture was lighted to give a bright orange lean flame. In order to avoid oxidation of carbon, the China dish with the burner was surrounded by perforated cardboard for flame enhancement. The soot particles were collected in an inverted glass collector, the inner walls of which had been wetted by benzene previously. A continuous bright flame is maintained till all the wax is completely utilized. A schematic diagram for collecting NiO-CNC is shown in Fig. 1. The entire process took about 2 h. Then the porcelain tile collector with NiO-CNC was scratched mechanically by a wooden spatula to collect the product, which was then stored in a desiccator.

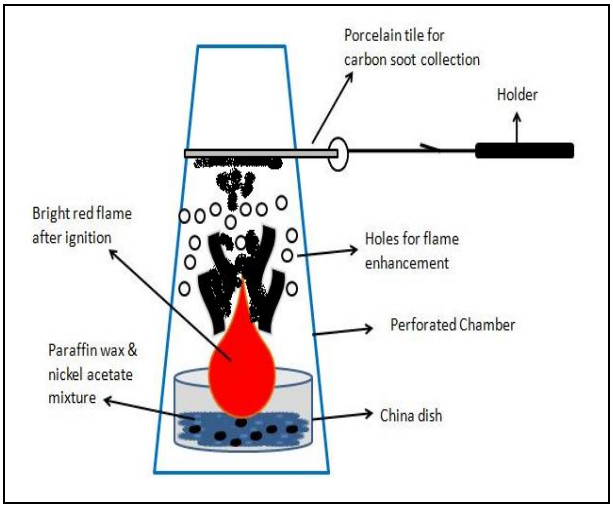

Fig. 1: Schematic diagram for the formation of NiO-CNC using Pyrolysis method

2.3 Preparation of Congo Red (CR) Dye Solution

Adsorption experiments were carried out with 250 ml conical flask using 100 ml of CR dye solution. 20 ml of desired concentration of dye solution was taken along with the appropriate amount of NiO-CNC adsorbent for complete adsorption to take place at 180 rpm agitation speed for the required time. The parameters influencing adsorption process were varied for each trial, such as solution pH (2 to 11), initial dye concentration (20, 40, 60, 80 and 100 mg/L), adsorbent dosage (20, 40, 60, 80 and 100 mg), contact time (0, 10, 20, 30, 40, 50 and 60 min) and temperature (303, 313, 323 and 333 K). After completion of each adsorption experiment, the samples were centrifuged and the concentration of the supernatant solution was analyzed using UV double beam spectro-photometer at wavelength, λ= 498 nm. All parameters were optimized separately, using the same procedure.

The percentage removal of the dye solution (R) and the adsorption capacity q_e were calculated using the equations (1) and (2):

$$R = \frac{(C_o - C_e)}{C_o} \times 100 \quad (1)$$

$$q_e = \frac{V(C_i - C_t)}{m}, \quad (2)$$

where, C_o is the initial dye concentration (mg/L), C_e is the concentration of dye solution at equilibrium, C_t is the concentration of the dye solution at the time (t), V is the volume of dye solution (L) and m is the amount of NiO-

CNC (g). All the experiments were repeated thrice, and their average was taken with minimum error (SSE ± 2).

3. RESULTS AND DISCUSSION

3.1 Characterization of Nickel Oxide Activated Carbon Nanocomposites

Figures 2 a and 2 b show low and high-resolution SEM images of NiO-CNC, respectively. The first picture shows a 51.28 nm cluster of tubular and spherical carbon particles. The latter, a high-resolution picture of the former, shows a carbon tube with brilliant oxide particles of around 50 nm in diameter along its walls.

The TEM image micrographs are shown in Fig. 3 (a-d), respectively. From Fig. 3 (a), it can be inferred that spherical particles are interconnected through carbon nanotubes resulting in the formation of clusters. The bridging of nanotubes results in the formation of a nanosphere with nickel oxide present inside it. The overlapping of the nanosphere results in the formation of CNT in which the nanosphere itself acts as a self-catalyst. It shows the carbonaceous material soot at 200 nm, and the nanomaterial obtained on burning paraffin wax is of spherical nature; NiO is embedded in the pores of the carbon matrix. The graphene layers of the carbon nanosphere, as seen in Fig. 3, are described by the lattice fringe (Fig. 3 c). The fringes are discovered to be non-uniform, and the crystalline is a reflection of the nanospheres' graphitization. The presence of diffraction rings and bight areas in the SAED patterns clearly demonstrated the particles' crystalline structure (Shooto and Dikio, 2011). The presence of pure carbon and nickel atoms can be seen clearly from the X-ray EDX analysis spectrum in Fig. 3 (d) without any contamination under the permissible limit (±0.01).

3.2 Size and Textural Morphology

The peaks at 37.26°, 43.90°, 64.28° and 77.41° correspond to (111), (200), (220) and (222) planes, (JCPDS Card No.: 47-1049) as a justification for the presence of NiO in NiO-CNC (Fig. 4). A broad peak between 20° to 30° plane indicated the presence of the hexagonal lattice of multi-walled carbon nanotubes (MWCNT) with the deposition of amorphous carbon (Langmuir, 1918; Freundlich, 1906; Adamson, 1997). The particle size of NiO-CNC was 50-58 nm in diameter, calculated using Scherrer's equation. The Raman spectrum of NiO-CNC is given in Fig. 5 with the range between 1000 to 2100 cm^{-1}. The peaks observed at 1310 and 1605 cm^{-1} correspond to the D-band and G-band, respectively. The D band is a breathing mode that depicts the disordered structures and edge planes as it is forbidden in a perfect single graphene layer. The D-band originates from the disorder in sp^2-hybridized carbon, thereby signifying the lattice distortions in curved graphene sheets, spheres, etc. Apparently, in the present study, the distortion was low due to the presence of sp^3-hybridized carbon. The G-band corresponds to the scattering of E_2g mode of the sp^2 atoms, with high intensities assigned to phonon mode of the single graphite layer seen in all the samples suggesting that NiO-CNC was composed of crystalline graphitic carbon.

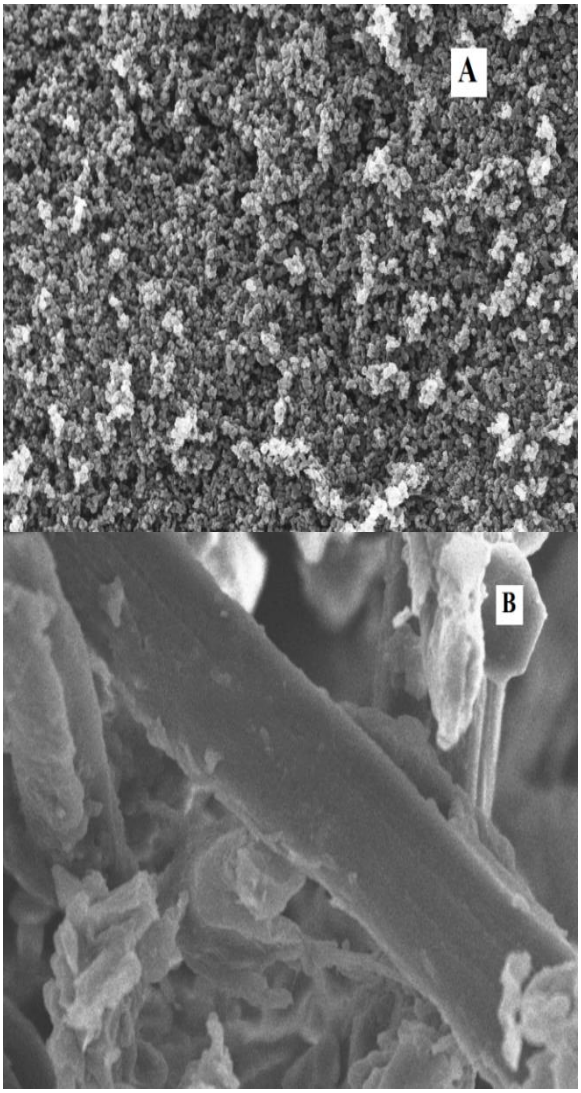

Fig. 2: (A) Field Emission Scanning Electron Microscopy (FE-SEM) of NiO-CNC and (B) Higher Magnification imaging of single CNT wrapped with NiO

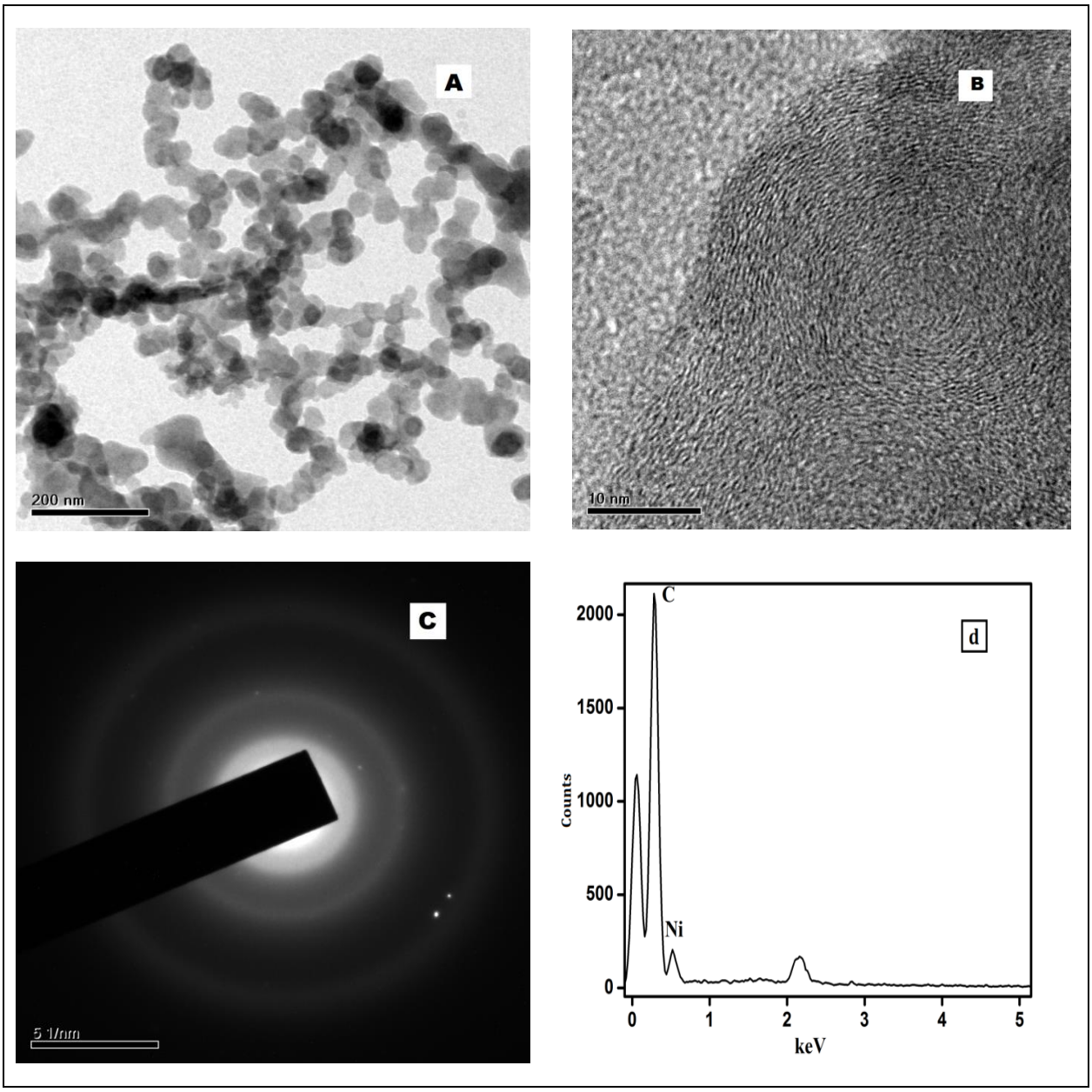

Fig. 3: (a) TEM imaging of NiO-CNC; (b) Higher Magnification Imaging of NiO-CNC; (c) SAED patterns of NiO-CNC and (d) EDAX spectra of NiO-CNC

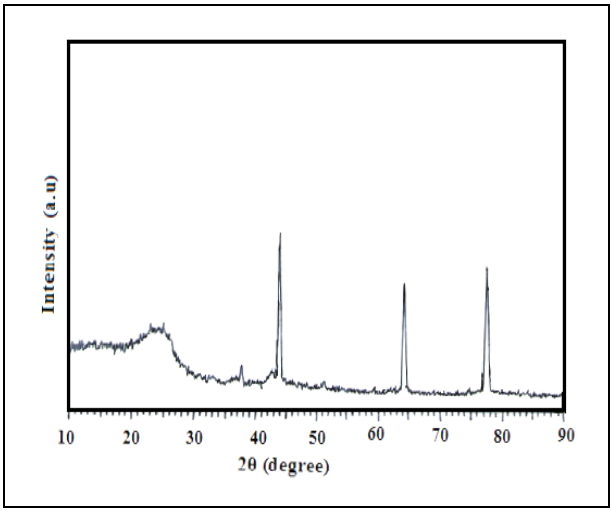

Fig. 4: XRD spectrum of NiO-CNC adsorbent

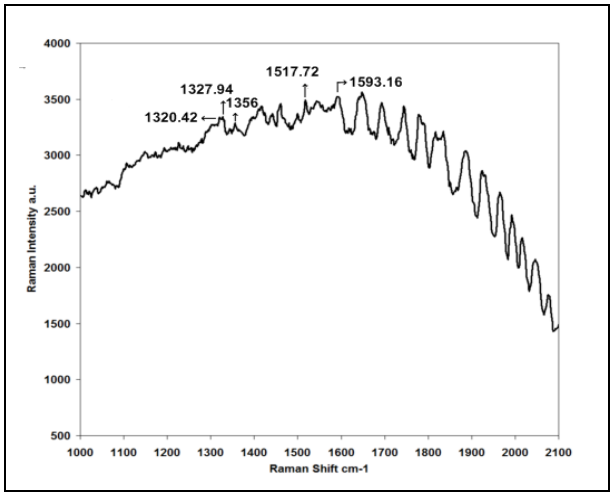

Fig. 5: Raman Spectrum of NiO-CNC adsorbent

3.3 Sorption Experimental Study

3.3.1 Effect of Time-dependent factor and solution pH onto CR sorption.

The influence of time-dependent behavior of CR dye sorption onto NiO-CNC was examined by varying the contact time (0-60 min), taking 20 ppm initial CR dye solution with 0.05 g of sorbent. There is a steady increase in dye removal with an increase in time (Fig 6). It was observed that 80% of dye removal was attained in 15 min. and maximum removal of 96% was obtained in 60 min., after which no further change was observed. Hence the optimized time of 60 min was selected for further studies. This is due to the fact that there were large numbers of vacant sites readily available for adsorption in 15 min and then the vacant sites were reduced gradually up to 60 min, and then there existed a repulsive force of attraction between the absorbed dye molecules on the NiO-CNC surface and solid phase (Dubinin and Radushkevich, 1947).

One of the most significant parameters which influence the amount of CR dye removal by NiO-CNC is solution pH. The influence of CR dye removal by NiO-CNC surface was analyzed with pH ranging 2-11, using an initial concentration of 20 ppm dye solution with 0.05 g of NiO-CNC dose under 60-minute (optimized) contact time. With the increase in pH, the adsorption increased gradually and reached a maximum at pH = 11. Maximum adsorption of 96.87 mg/g was obtained for CR removal using NiO-CNC adsorbent (Fig. 6).

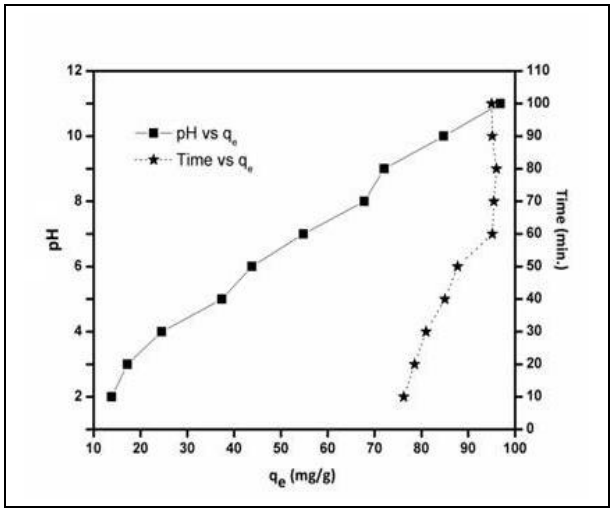

Fig. 6: Effect of solution pH and time-dependent factor on CR removal by NiO-CNC (initial CR dye concentration: 100 mg/l, NiO-CNC dose: 20 mg, sample solution: 20 ml, variable time period: 0-60 min, variable solution pH: 2-11 and temperature: 30 °C)

The pH dependency of adsorption efficiency could be explained by the functional groups involved in dye uptake and dye chemistry. Maximum dye removal was attained in the basic medium at a pH 11. Formation of hydroxide dominates, leading to the binding interaction with the competition between Ni^{2+} of the adsorbent and Na^{+} ion in the dye resulting in the formation of NaOH. This led to the replacement of Ni^{2+} over Na^{+}, as evident from the mechanism. A comparison of sorption isotherms of CR onto various sorbents are listed in Table 1.

3.3.2 Effect of initial dye concentration and sorbent amount onto CR sorption

The influence of initial CR concentration using NiO-CNC was studied and represented in Fig. 7. From the experimental results obtained for CR removal using NiO-CNC with varying CR dye concentration (20-100 mg/L) with the adsorbent (0.05 g), it has been concluded that rapid removal occurred in the initial stage, due to the binding of CR dye and a greater number of sites were available for adsorption. At equilibrium, saturation

occurred due to the complete occupation of sites on adsorption.

The amount of NiO-CNC adsorbent amount also plays a vital role in deciding the cost-effectiveness of the process. The effect of NiO-CNC dose on CR dye removal is also shown in Fig. 7. It is evident from the figure that the increase in CR dye was rapid with an increase in NiO-CNC amount; but no change was observed beyond the dose of 5g/L; this was because of the absence of available sites and exchanging of ions in the adsorption process.

3.4.1 Two-parameter isotherm model

Maximum sorption occurs when a saturated monolayer of the solute molecules binds with the surface of the sorbent; no migration of sorbate molecule on the surface plane and the sorption energy is constant. The non-linear form of the Langmuir isotherm model (1918) is expressed as follows:

$$q_e = \frac{q_{max} b_L C_e}{1 + b_L C_e} \quad (3)$$

where, q_e is the amount of metal adsorbed (mg/g) and C_e is the equilibrium concentration of the solution (mg/L). q_m and b_L are the Langmuir constants indicating the adsorption capacity and energy, respectively. The essential feature of the Langmuir model can be expressed in terms of a dimensionless constant separation factor (R_L):

$$R_L = 1/1+(1+K_L C_o) \quad (4)$$

where, K_L is the Langmuir constant (L/mg) and C_o is initial concentration (mg/L).

Freundlich isotherm (1906) is the earliest known relationship describing the non-ideal and reversible adsorption, not restricted to the formation of a monolayer. This empirical model can be applied to multilayer adsorption, with non-uniform distribution of adsorption heat and affinities over the heterogeneous surface (Adamson and Gast, 1997). The non-linear form of Freundlich isotherm is represented as

$$q_e = K_f C_e^{1/n} \quad (5)$$

where, K_F is the Freundlich isotherm constant ((mg/g). n=adsorption intensity, C_e= equilibrium concentration of adsorbate (mg/L) and q_e = the amount of metal adsorbed of the adsorbent at equilibrium.

The Temkin isotherm (1940) model explicitly defines the interactions between adsorbent and adsorbate. The following conditions are assumed in this model: (i) because of adsorbent–adsorbate interactions, the heat of adsorption of all molecules in the layer reduces linearly with coverage and (ii) a homogeneous distribution of binding energies, up to a maximum binding energy, characterises adsorption. The Temkin isotherm is derived on the assumption that the decrease in sorption heat is linear rather than logarithmic, as predicted by the Freundlich equation. The non-linear form of Temkin isotherm is represented as,

$$q_e = B_T \ln(AC_e) \quad (6)$$

where, B_T = RT/b is the constant related to the heat of adsorption, b is the heat of adsorption (kJ/mol), R is the gas constant (8.314 J/mol.K), T is the temperature (K), and A is the adsorption equilibrium binding constant related to the maximum binding energy (L/mg).

Table 1. Comparison of sorption isotherms onto various sorbents

Adsorbents	Isotherm	q_e (mg/g)	References
Chitosan hydro beads	Langmuir	92.59	Chatterjee *et al.* 2007
Coal-based Activated carbon	Langmuir	52	Grabowska and Gryglewicz, 2007
Cashew nutshell	Langmuir	5.18	Kumar et al. 2010
Cashew nut shell	Freundlich	1.35	Kumar et al. 2010
Kaolin	Fruendlich	1.98	Vimonses *et al.* 2009
Raw pine cone	Freundlich	19.18	Dawood and Sen, 2012
Acid-treated pine cone	Experimental	40.19	Dawood and Sen, 2012
NiO-CNC	Langmuir	95.02	Present Study

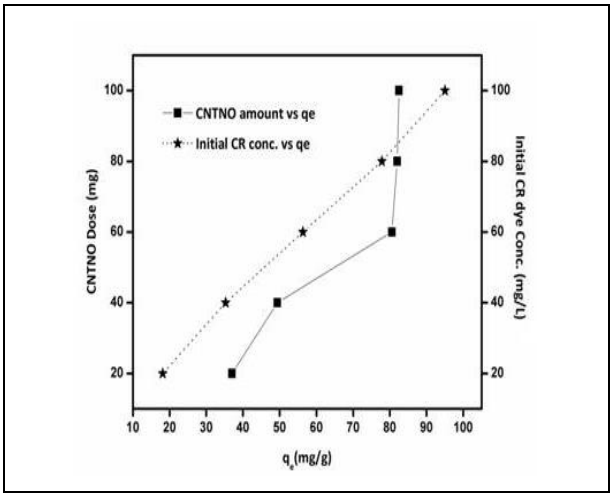

Fig. 7: Effect of NiO-CNC dose and initial concentration on CR removal by NiO-CNC (solution pH: 11, equilibrium time: 60 min, sample solution: 20 ml, variable initial CR concentration: 20-100 mg/l, variable NiO-CNC dose: 20-100 mg and temperature: 30 °C)

3.4 Sorption Isotherm

A sorption isotherm is a relationship between equilibrium sorption capacity and equilibrium concentration at a certain temperature. To determine the sorption capacity of NiO-CNC and design of the process, isotherms were obtained at 303, 313, 323 and 333 K, respectively. q_e is the sorption capacity (mg/g); C_e is the equilibrium concentration (mg/L). A plot of C_e vs. q_e is plotted with 2-parameter and 3-parameter non-linear isotherm models using MATLAB 7.1 to find out the best suitable fitting model. The experimental data were plotted with 2-parameter models: Langmuir (1918) and Freundlich (1906), Temkin (1940) and Dubinin-Radushkevich (1947) and 3-parameter models: Redlich-Peterson (1959), Sips (1948), Khan (1997) and Toth (1971) models (Fig. 8 and 9 (A-D)) The parameter constants, co-relation co-efficient, sum of error squared (SSE) and root mean square (RMSE) were summarized (Table 1.)

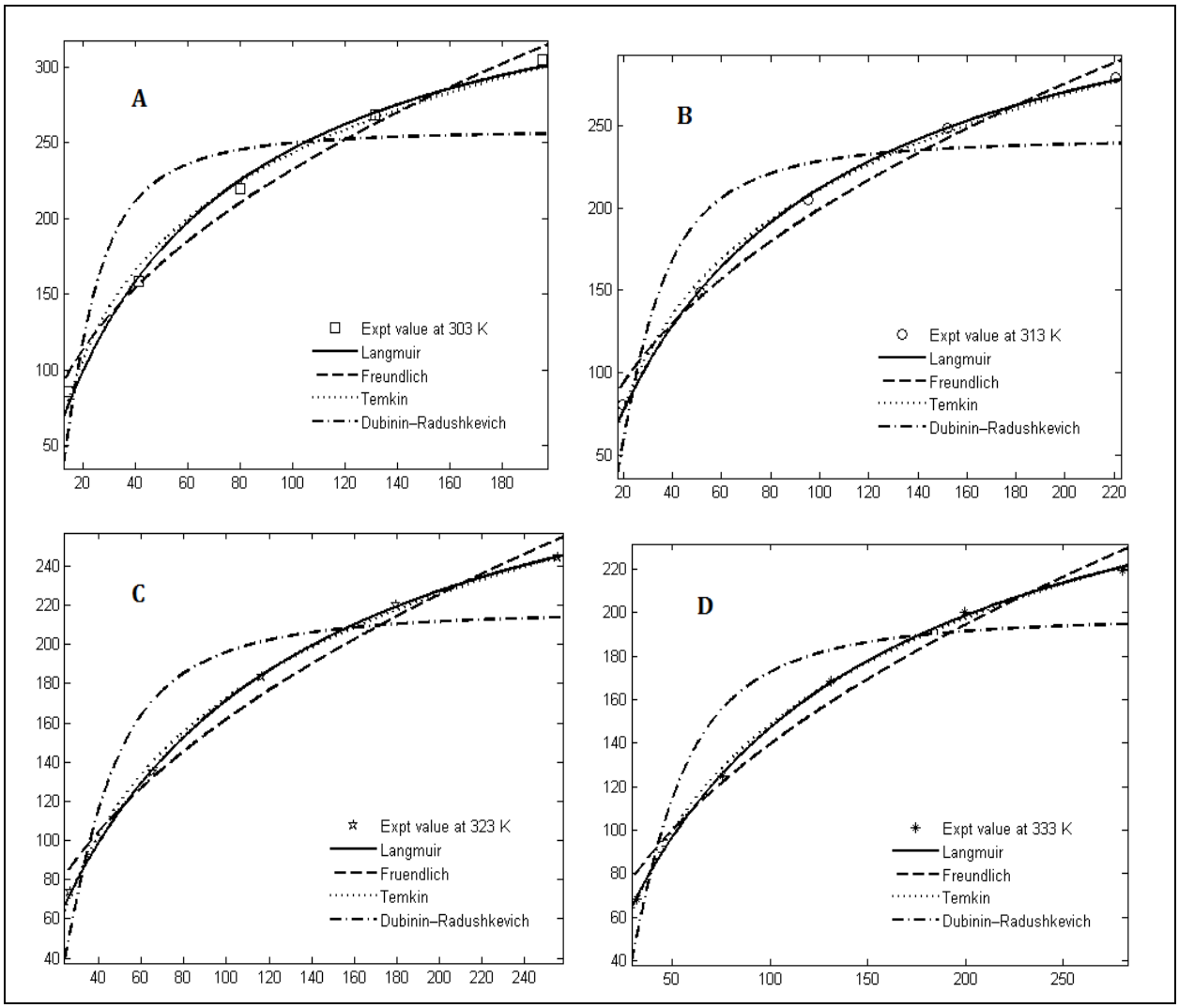

Fig. 8 (A-D): Non-linear 2-parameter isotherm model of NiO-CNC sorbent with temperature variation gradient

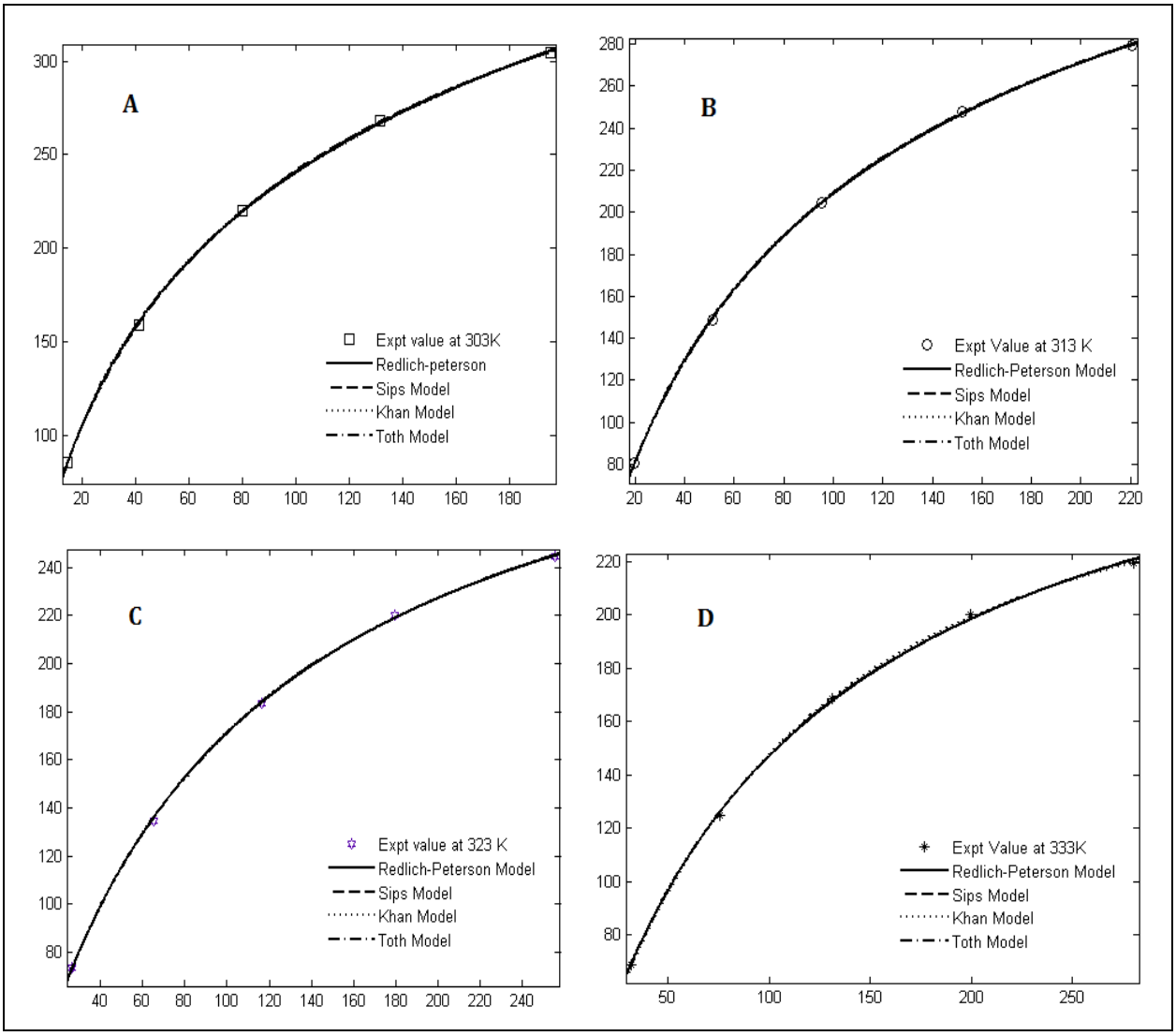

Fig. 9 (A-D): Non-linear 3-parameter isotherm model of NiO-CNC sorbent with temperature variation gradient

The Dubinin-Radushkevich isotherm (1947) was developed to explain the adsorption of subcritical vapours onto micropore materials *via* a pore-filling process. It is commonly used to explain the adsorption mechanism onto a heterogeneous surface with a Gaussian energy distribution (Gunay, 2007). (Dabrowski, 2001). The Dubinin-Radushkevich isotherm's non-linear form is written as,

$$q_e = q_m \exp\left(-\beta\left(RT \ln\left(1+\frac{1}{C_e}\right)\right)^2\right) \quad (7)$$

where, q_e = amount of adsorbate in the adsorbent at equilibrium (mg/g), C_e = equilibrium concentration of adsorbate (mg/L), q_m is the Dubinin-Radushkevich monolayer capacity (mg/g), β is a constant related to sorption energy (mean free energy), R is the gas constant (8.314 J/mol K) and T is the absolute temperature.

$$E = \frac{1}{\sqrt{2\beta}} \quad (8)$$

When one mole of ions is transported to the adsorbent surface, the value of E is less than 8 kJ/mol, indicating physical adsorption (Benito, 2009). The value of E is between 8 and 16 kJ/mol indicates that the adsorption process follows ion-exchange (Liu *et al.* 2003), while its value in the range of 20-40 kJ/mol indicates chemisorption (Shao *et al.* 2000).

The (theoretical) q_{max} value was found to be almost similar to the experimental value obtained from the studies. The adsorption process was found to be exothermic, and the q_e values were found to be in the decreasing order with an increase in temperature gradient. The R^2 values of Langmuir isotherm were in the order of 0.9956, 0.9986, 0.9998 and 0.9996 with an increase in temperature from 30 °C, 40 °C, 50 °C and 60 °C; thus, the Langmuir isotherm fits well with the

obtained equilibrium data. The value of n > 1, from the Freundlich isotherm, indicated that the process is physical adsorption. The values of A and B constants of Temkin isotherm were in the range of 0.1-0.08 and 36-30 in the decreasing order with an increase in temperature. The Dubinin-Radushkevich isotherm value, q_m, is 258.1 mg/g, β is 9.97×10^{-8} mg^2/J^2 and the magnitude of E = 22.34 of at 30 °C, indicating that the reaction followed chemisorption. Thus, both physical adsorption and chemical adsorption were taking place simultaneously, which resulted in the increased dye removal by the adsorbent NiO-CNC. The non-linear isotherm parameters obtained using 2-parameter models with temperature gradient are listed in Table 2.

Table 2. Non-linear isotherm parameters obtained on CR removal using NiO-CNC using 2-parameter models with a temperature gradient

2-parameter Isotherm model	Parameters and constants	Congo red removal			
		30 °C	40 °C	50 °C	60 °C
Langmuir	q_m (mg/g)	390.6	373.1	337.6	305.9
	k_L(L/mg)	0.01701	0.01312	0.01033	0.00925
	R^2	0.9956	0.9986	0.9998	0.9996
	SSE	133.2	34.82	3.609	6.417
	RMSE	6.664	3.407	1.097	1.463
Freundlich	K_f [((mg/g) (L/mg) (1/n))]	29.55	23.14	17.8	15.38
	n (g/L)	2.234	2.14	2.086	2.088
	R^2	0.9885	0.9853	0.9805	0.9757
	SSE	349.5	369.9	366.8	358.2
	RMSE	10.79	11.1	11.06	10.93
Temkin	A (constant)	0.1765	0.128	0.09533	0.08253
	B (constant)	36.77	35.95	33.25	30.55
	R^2	0.9943	0.9963	0.9978	0.998
	SSE	173.9	93.8	41.66	28.77
	RMSE	7.614	5.592	3.726	3.097
Dubinin-Radushkevich	q_m (mg/g)	258.1	242	217.2	198.1
	B (mg^2/J^2)	0.000997	0.001792	0.003127	0.004209
	R2	0.7715	0.8026	0.8343	0.8541
	E	22.37	17.06	12.64	10.9
	SSE	6974	4977	3114	2152
	RMSE	48.22	40.73	32.22	26.78

3.4.2 Three-parameter model

The Langmuir and Freundlich models are combined in the Redlich-Peterson isotherm (1959). It approaches the Freundlich model at greater concentrations and agrees with the Langmuir equation's lower concentration limit. The Redlich-Peterson isotherm model has a non-linear form as follows:

$$q_e = \frac{K_R C_e}{1+\alpha_R C_e^{\beta}} \qquad (9)$$

where, q_e is the amount of adsorbate in the sorbent at equilibrium (mg/g), C_e is the equilibrium concentration (mg/L); K_R is the Redlich - Peterson isotherm constant (L/g), α_R is the Redlich - Peterson isotherm constant (L/mg) and β is the exponent, which lies between 0 and 1; if β nearer to 1, Langmuir isotherm is preferable, and if β is nearer to 0, Freundlich is preferable.

Sips isotherm (1948) is a hybrid form of Langmuir and Freundlich expressions deduced for forecasting heterogeneous adsorption systems (2007) and avoiding the Freundlich isotherm model's limitation of growing adsorbate concentration. It lowers to the Freundlich isotherm at low adsorbate concentrations. It predicts a mono-layer adsorption capacity characteristic of the Langmuir isotherm at high concentrations. The Sips Model's non-linear version is written as,

$$q_e = \frac{q_m K_s C_e^{n_s}}{1+a_s C_e^{n_s}} \qquad (10)$$

where, K_s is the equilibrium constant; if the value of n_s is equal to 1, then this equation will become a Langmuir equation. Alternatively, as either C_e or a_s approaches 0, the isotherm follows the Freundlich model.

Khan isotherm model (1997) is generally suggested for pure solutions. The non-linear form of Khan Model is expressed as,

$$q_e = \frac{(q_m b_k C_e)}{(1 + b_k C_e)^{a_k}} \quad (11)$$

where, b_k is the Khan's model constant and a_k is the Khan's model exponent.

Toth isotherm model (1971) is another empirical equation developed to improve Langmuir isotherm fittings (experimental data) and useful in describing heterogeneous adsorption systems, satisfying both low and high-end boundaries of the concentration (2006). The non-linear form of the Toth Model is expressed as,

$$q_e = \frac{F b_T C_e}{\left[1 + (b_T C_e)^{1/n}\right]^n} \quad (12)$$

where, b_T is the Toth model's constant, and n is the Toth model's exponent ($0 < n \leq 1$).

The exponents, constants and parameter values are given in Table 3 with a temperature gradient. From the results, sorption takes place effectively at room temperature suggesting that the sorption was more feasible and exothermic. The Redlich-Peterson parameters - K_R is 9.417 (L/g), α_R is 0.0702 (L/mg) and B_R is 0.8106 nearer to 1, indicate that Langmuir fits well with the obtained experimental data. The values from the Sips isotherm, a_s and n_s, were 0.0098 and 0.7834, respectively. The value of n_s was approaching 1, indicating Langmuir isotherm fits well. The q_{max} value from Khan Model was 191.8 mg/g. The constants a_k and b_k were 0.7453 and 0.0440. The value of F is 578.6 mg/g and constants b_T and n were 9.624 and 0.5807, respectively.

3.4.3 Comparison of isotherms

Considering the relative errors, parameters and the constants from the 2-parameter and the 3-parameter isotherm models, the R^2 values were in the range of Langmuir > Temkin > Freundlich > Dubinin-Radushkevich and in the case of 2-parameter isotherm models and in 3-parameter isotherm models, Toth > Sips > Redlich-Peterson > Khan. However, the results of the non-linear regression analysis indicate that the 3-parameter isotherm model has no noticeable change in the CR-NiO-CNC sorption system. The correlation of the experimental data with these isotherm models implied that both mono-layer and heterogeneous surfaces exist under the experimental conditions studied. Langmuir isotherm was fitting well, suggesting that the dye molecules were binding on the pores and walls of the nanosphere with physisorption as the predominating mechanism along with the chemical interaction suggesting that the adsorption mechanism was complex.

3.5 A Single-stage Batch Adsorber Design

The batch adsorber for dye expulsion from the dye solution was designed using the best-fitted adsorption isotherm model. Fig. 10 shows the batch adsorber from a schematic view. The objective purpose of the current adsorber was to quantify the adsorbent measure, which is a necessity for treating the known volume and concentration of the CR dye from the aqueous under ideal conditions. The material balance for the batch adsorber is given as follows:

$$V\,(C_o - C_e) = M(q_e - q_o) \quad (13)$$

where, V is the volume of copper ions solution (L), C_o is the initial copper ions concentration (mg/L), C_e is the copper ions concentration at equilibrium (mg/L), M is the mass of the adsorbent (g), q_e is the equilibrium adsorption capacity (mg/g) and q_o is the adsorption capacity at time t = 0 (mg/g). The fresh adsorbent was used for the present adsorption system; hence, q_o = 0 and Eq. (13) can be rewritten as:

$$M = \frac{(C_o - C_e)}{q_e} V \quad (14)$$

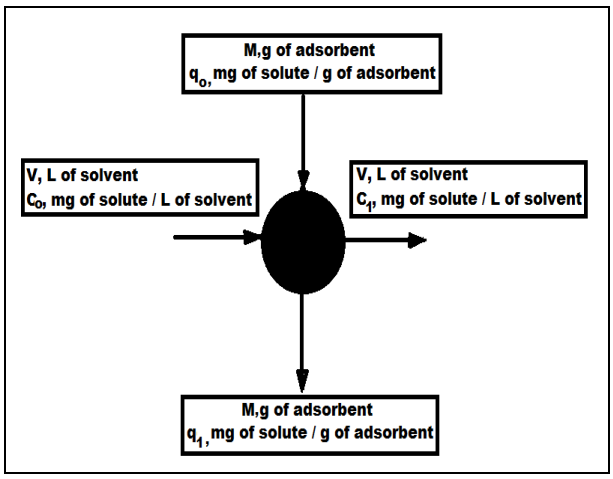

Fig. 10: Single-stage batch adsorber design

Table 3. Non-linear isotherm parameters obtained on CR removal using NiO-CNC using 3-parameter models with a temperature gradient

3-parameter Isotherm Models	Parameters and constants	Congo red removal			
		303 K	313 K	323 K	333 K
Redlich-Peterson Model	K_{RP} (L/g)	9.417	5.822	3.56	2.831
	α_{RP} (L/mg)	0.0702	0.03094	0.011 74	0.009256
	β_{RP}	0.8106	0.8809	0.9817	1
	R^2	0.9998	0.9998	0.9998	0.9996
	SSE	6.161	4.159	3.184	6.417
	RMSE	1.755	1.422	1.262	1.463
Sips Model	K_s $(mg/L)^{-1/n}$	12.77	7.41	3.824	2.831
	β_s	0.7834	0.8728	0.9736	1
	a_s	0.0098	0.009698	0.009794	0.009256
	R^2	0.9999	0.9999	0.9999	0.9996
	SSE	0.7209	1.18	2.631	6.417
	RMSE	0.6004	0.7681	1.147	1.463
Khan Model	Q_{max} (mg/g)	191.8	244.4	321.4	305.9
	b_k	0.04403	0.02248	0.01096	0.009256
	a_k	0.7453	0.8209	0.9746	1
	R^2	0.9997	0.9998	0.9998	0.9998
	SSE	10.18	6.056	3.373	2.4
	RMSE	2.256	1.74	1.299	1.095
Toth Model	F (mg/g)	578.7	455	347.7	308.4
	g	9.624	23.89	77.34	100
	d	0.5807	0.7424	0.9522	0.9845
	R^2	0.9999	0.9999	0.9998	0.9995
	SSE	2.545	2.395	2.926	7.249
	RMSE	1.128	1.094	1.21	1.554

The best-obeyed adsorption isotherm for the present adsorption framework was the Langmuir model. This model can be incorporated into Eq. (14) and the condition can be changed as:

$$M = \frac{(C_o - C_e)(1 + K_L C_e)}{q_m K_L C_e} V \qquad (15)$$

Eq. (15) relates the mass of adsorbent with the volume of the CR dye solution for the initial concentration of dye solution at a constant temperature. The adsorption isotherm information was fitted to Eq. (15) and the outcomes were depicted in Fig. 11.

3.6 Sorption Kinetics

Several models were proposed to express the mechanism between the solute sorption and the sorbent. To investigate the mechanism of sorption by NiO-CNC onto CR dye removal, parameter constants were calculated using pseudo-first order (Sips, 1948), pseudo-second order (Gunay, 2007), Elvolich (Khan *et al.* 1997) and Intra-particle diffusion (Toth, 1971) equations. The linear form of pseudo-first order model (Eqn. 16) is as follows,

$$\log (q_e - q_t) = \log q_e - K_{1\text{-}ad}\, t / 2.303 \qquad (16)$$

where, $K_{1\text{-}ad}$, q_t and q_e are the pseudo-first order equilibrium rate constant (1/min), amount of dye adsorbed at time t (mg/g) and amount of CR dye adsorbed at equilibrium time t (mg/g). Linear plot of ln $(q_e\text{-}q_t)$ against contact time t is plotted. (Fig 12).

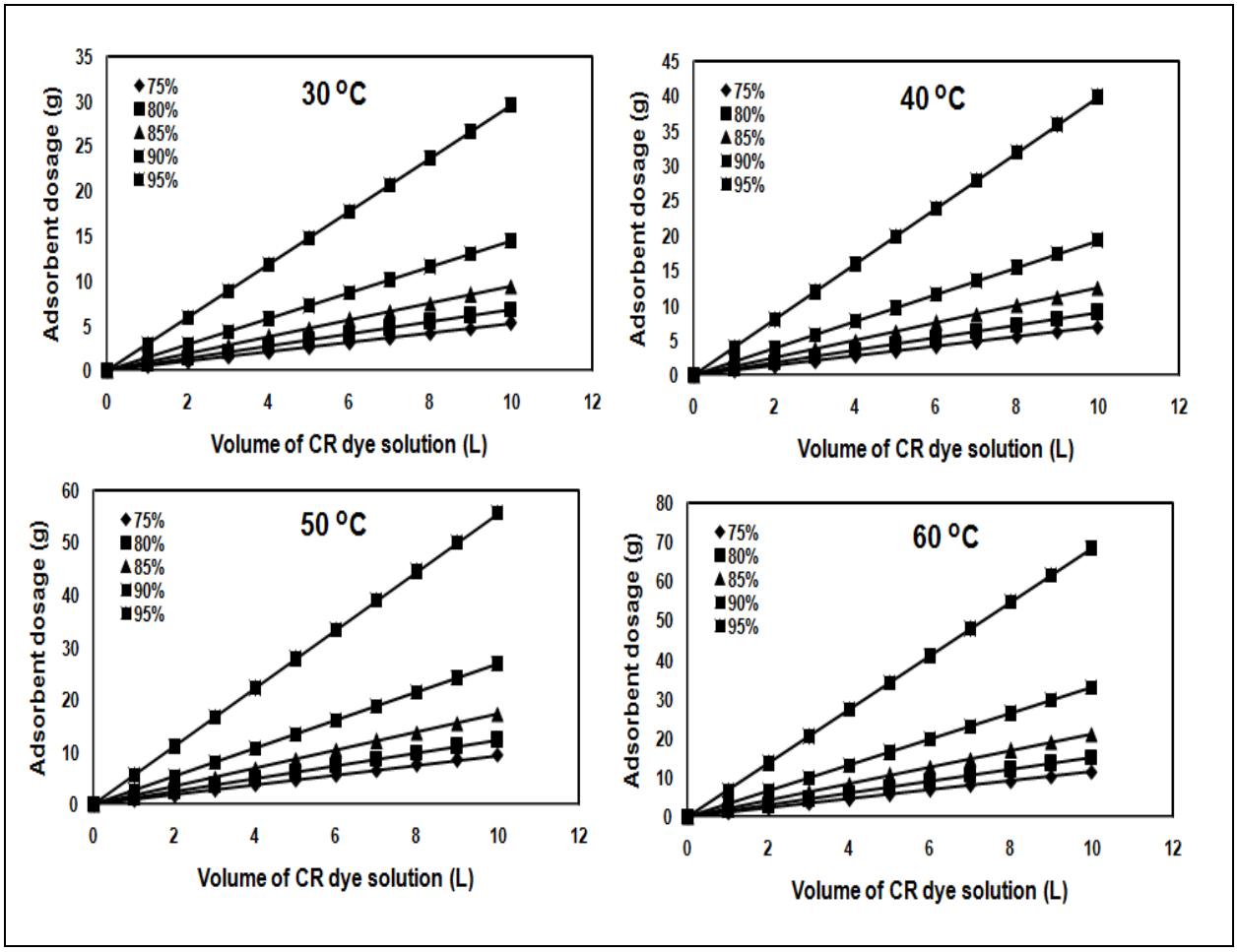

Fig. 11: Adsorber design results for the removal of CR dye by NiO-CNC

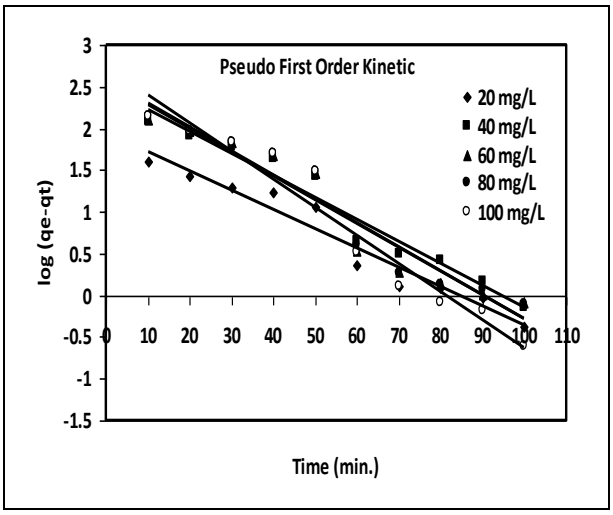

Fig. 12: Pseudo-first order kinetic model of NiO-CNC onto CR removal with concentration gradient at 30 °C

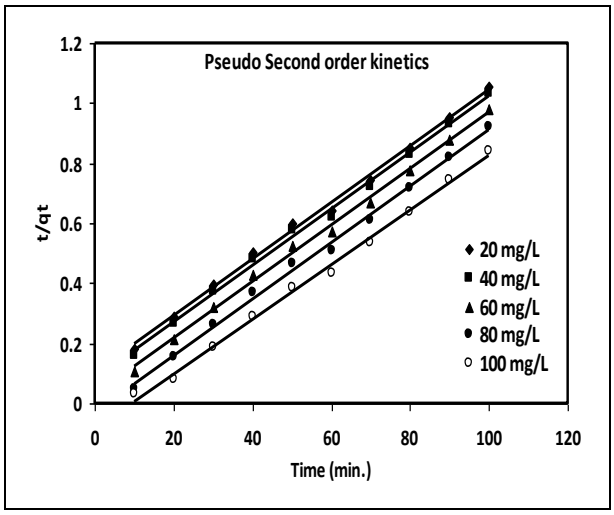

Fig. 13: Pseudo-second order kinetic model of NiO-CNC onto CR removal with concentration gradient at 30 °C

The linear form of the pseudo-second order model (Eqn. 17) is as follows,

$$\frac{t}{q_t} = \frac{1}{k_2 q_e^2} + \frac{1}{q_e} t \quad (17)$$

where, k_2 is the pseudo-second order sorption rate constant (g/(mg.min)), q_e and q_t are same as above. A linear plot of t/q_t against t was plotted. (Fig. 13).

From the studies, it was clearly evident that the reaction follows pseudo-second order kinetics from the values of co-relation co-coefficient $R^2 \geq 0 \leq 1$. The experimental sorption capacity, q_e values, were fitting well, close to the observed theoretical one. The obtained rate constants and parameter constants shown in Table 4 confirmed that the pseudo-second order model was a good fit in the adsorption process.

3.6 Thermodynamic Test

The thermodynamic parameters, such as standard free energy change (ΔG°), enthalpy change (ΔH°) and entropy change (ΔS°) have been estimated to evaluate the feasibility of the adsorption process.

$$K_c = \frac{C_{Ae}}{C_e} \quad (18)$$

$$\Delta G^o = -RT \ln K_c \quad (19)$$

$$\log K_c = \frac{\Delta S^o}{2.303R} - \frac{\Delta H^o}{2.303RT} \quad (20)$$

where, K_c is the adsorption equilibrium constant, C_{Ae} is the amount of metal ions adsorbed onto the adsorbent per liter of solution at equilibrium (mg/L), C_e is the concentration of metal ions in the solution at equilibrium (mg/L), R is the gas constant (8.314 J/mol.K) and T is the temperature (K). The observed thermodynamic data for the removal of CR dye using NiO-CNC was made to fit with the equations (18) and (19). A plot of K_c against 1/T was plotted (Fig. 14) and the results were tabulated (Table 5). The values were found to be decreasing with an increase in temperature, indicating that the adsorption process was more feasible at low temperatures. The negative ΔG values indicated that the adsorption process was more feasible and spontaneous. The negative ΔH value indicated that the process was exothermic and entropy change (ΔS) implied that the adsorption process was randomization at CR/NiO-CNC interface.

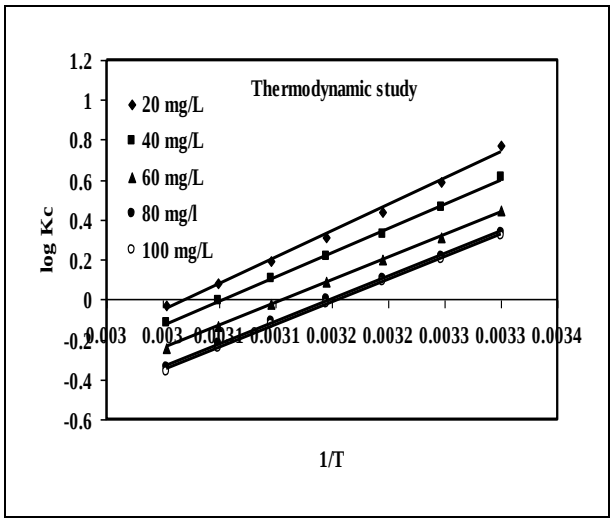

Fig. 14: Van-Hoff plot for thermodynamic studies on CR removal

Table 4. Kinetic parameters and constants on CR removal using NiO-CNC at 30 °C

Kinetic Model	Parameters	Initial concentration of CR dye solutions (mg/L)				
		20	40	60	80	100
Pseudo-first order model	k_{ad} (min^{-1})	1.74×10^{-4}	1.99×10^{-4}	2.15×10^{-4}	2.18×10^{-4}	2.55×10^{-4}
	q_e, cal (mg/g)	6.64	9.12	9.40	9.51	10.05
	R^2	0.9497	0.9622	0.9367	0.9363	0.9483
Pseudo-second order model	k (g $mg^{-1}min^{-1}$)	3.22×10^{-4}	3.21×10^{-4}	3.23×10^{-4}	3.19×10^{-4}	3.32×10^{-4}
	q_e cal (mg. g^{-1})	14.38	31.8	49.78	69.25	91.89
	qe expt. (mg. g^{-1})	18.12	35.26	56.31	77.83	95.02
	h(mg.g^{-1}.min^{-1})	9.727	12.30	34.36	32.36	11.97
	R^2	0.9968	0.9969	0.9961	0.9968	0.9960

Table 5. Thermodynamic parameters and constants of NiO-CNC sorbent at 30 °C

Congo red Conc. (mg/L)	ΔHº (kJ/mol)	ΔSº (J/mol/K)	ΔGº (kJ/mol)						
			303 K	308 K	313 K	318 K	323 K	328 K	333 K
20 mg/L	-50.55	-153.02	-1.950	-1.502	-1.139	-0.818	-0.518	-0.218	-0.0755
40 mg/L	-46.53	-142.11	-1.552	-1.183	-0.861	-0.563	-0.274	-0.023	0.032
60 mg/L	-43.76	-135.93	-1.120	-0.807	-0.516	-0.233	0.513	0.354	0.670
80 mg/L	-43.19	-135.96	-0.852	-0.562	-0.282	-0.002	0.287	0.602	0.941
100 mg/L	-43.22	-136.41	-0.797	-0.510	-0.232	0.048	0.338	0.657	1.002

4. CONCLUSION

The present study was focused upon the synthesis of MWCNT using paraffin wax with the incorporation of NiO by using nickel acetate as a catalyst by the combustion process. The synthesized NiO-wrapped MWNTs were tested for suitability as an adsorbent for the removal of Congo red dye in an aqueous medium. The adsorption equilibrium parameters such as solution pH, contact time, NiO-CNC dosage and initial CR dye concentration were evaluated to find out the optimized conditions for the feasible nature of the process. The maximum removal of 80% was observed under a pH of 11, a dosage of 5 g/L and an initial CR dye concentration of 100 mg/L, with a time period of 60 minutes. The obtained equilibrium data was fitting well with the Langmuir model. The negative ΔG, ΔH and ΔS values implied that the adsorption was feasible, exothermic and spontaneous. Overall results have suggested that MWCNT/NiO was an effective adsorbent for the removal of dyes from textile effluents.

FUNDING

This research received no specific grant from any funding agency in the public, commercial, or not-for-profit sectors.

CONFLICTS OF INTEREST

The authors declare that there is no conflict of interest.

COPYRIGHT

This article is an open access article distributed under the terms and conditions of the Creative Commons Attribution (CC-BY) license (http://creativecommons.org/licenses/by/4.0/).

REFERENCES

Adamson, A. W. and Gast, A. P., Wiley Interscience, New York, (1997).

Benito, P., Herrero, M., Labajos, F. M., Rives, V., Royo, C., Latorre, N. and Monzon, A., Production of carbon nanotubes from methane: Use of CO-Zn-Al catalysts prepared by microwave-assisted synthesis, *Chem. Eng. J.*, 149(1-3), 455-462(2009). https://doi.org/10.1016/j.cej.2009.02.022

Dabrowski, A., Adsorption-from theory to practice, *Adv. Colloid Interface Sci.*, 93(1-3), 135–224(2001).

Das, R., Hamid, S. B. A., Ali, M. E., Ismail, A. F., Annuar, M. S. M. and Ramakrishna, S., Multifunctional carbon nanotubes in water treatment: The present, past and future, *Desal.* 354, 160–179(2014). https://doi.org/10.1016/j.desal.2014.09.032

Dikio, E. D. and Bixa, N., Carbon nanotubes synthesis by catalytic decomposition of ethyne using Fe/Ni catalyst on aluminium oxide support, *Int. J. Appl. Chem.*, 7(1), 35-42(2011).

Dikio, E. D., Thema, F. T., Dikio, C. W. and Mtunzi, F. M., Synthesis of carbon nanotubes by catalytic decomposition of ethyne using Co-Zn-Al catalyst, *Int. J. Nanotech. Appl.*, 4(2), 117(2010).

Dubinin, M. M. and Radushkevich, L. V., Equation of the characteristic curve of activated charcoal, *Chem. Zentr.*, 1, 875–890(1947).

Farhat, S. and Scott, S. D., Review of the arc process modeling for fullerence and nanotubes production, *J. Nanosci. Nanotechnol.*, 6 (5), 1189–1210(2006). https://doi.org/10.1166/jnn.2006.331

Freundlich, H. M. F., Over the adsorption in solution, *J. Phy. Chem.*, 57, 385–470(1906).

Ghaedi, A. M., Ghaedi, M., Vafaei, A., Iravani, N., Keshavarz, M., Rad, M., Tyagi, I., Agarwal, S. and Gupta, V. K., Adsorption of copper(II) using modified activated carbon prepared from pomegranate wood; Optimization by bee algorithm and response surface methodology, *J. Mol. Liq.*, 206, 195–206(2015). https://doi.org/10.1016/j.molliq.2015.02.029

Gong, J. L., Wang, B., Zeng, G. M., Yang, C. P., Niu, C. G., Niu, Q. Y. and Liang, Y., Removal of cationic dyes from aqueous solution using magnetic multi-wall carbon nanotubes nanocomposite as adsorbent, *J. Hazard. Mater*., 164(2-3), 1517–1522(2009). https://doi.org/10.1016/j.jhazmat.2008.09.072

Gunay, A., Arslankaya, E. and Tosun, I., Lead removal from aqueous solution by natural and pretreated clinoptilolite: Adsorption equilibrium and kinetics, *J. Hazard. Mater*., 146(1-2), 362–371(2007).

Gupta, V. K. and Saleh, T. A., Sorption of pollutants by porous carbon, carbon nanotubes and fullerene – An overview, *Environ. Sci. Pollut. Res*., 20(5), 2828–2843(2013a). https://doi.org/10.1007/s11356-013-1524-1

Gupta, V. K., Agarwal, S. and Saleh, T. A., Synthesis and characterization of alumina-coated carbon nanotubes and their application for lead removal, *J. Hazard. Mater.*, 185, 17–23(2011). https://doi.org/10.1016/j.jhazmat.2010.08.053

Gupta, V. K., Kumar,R., Nayak, A, Saleh, T. A. and Barakat, M. A., Adsorptive removal of dyes from aqueous solution onto carbon nanotubes: A review, Adv. Colloid Interf. Sci. 193-194, 24–34(2013b). https://doi.org/10.1016/j.cis.2013.03.003

Gupta, V. K., Sadegh, H., Yari, M., Shahryari-Ghoshekandi, R., Maazinejad, B. and Chahardori, M., Removal of ammonium ions from wastewater: A short review in development of efficient methods, Glob. *J. Environ. Sci. Manag*., 1(2), 149–158(2015). https://doi.org/10.7508/GJESM.2015.02.007

Gupta, V. K., Tyagi, I., Agarwal, S., Sadegh, H., Shahryari-Ghoshekandi, R., Yari, M. and Yousefi-Nejat, O., Experimental study of surfaces of hydrogel polymers HEMA, HEMA-EEMA-MA and PVA as adsorbent for removal of azo dyes from liquid phase, *J. Mol. Liq*., 206, 129–136(2015).

Iijima, S. and Ichihashi, T., Single-shell carbon nanotubes of 1-nm diameter, *Nature*, 363, 603–605(1993). https://doi.org/10.1038/363603a0

Iijima, S., Helical microtubules of graphitic carbon, Nature, 354 (6348) 56–58(1991). https://doi.org/10.1038/354056a0

Jin, W. J., Jeon, H. J., Kim, J. H., Youk, J. H., A study on the preparation of poly(vinyl alcohol) nanofibers containing silver nanoparticles, *Synth. Met*. 157(10-12), 454 – 459(2007). https://doi.org/10.1016/j.synthmet.2007.05.011

Khan, A. R., Ataullah, R. and Al-Haddad, A., Equilibrium adsorption studies of some aromatic pollutants from dilute aqueous solutions on activated carbon at different temperatures, *J. Colloid Interface Sci.*, 194(1), 154–165(1997). https://doi.org/10.1006/jcis.1997.5041

Kirupha, S. D., Kalaivani, S., Vidhyadevi, T., Premkumar, M. P., Baskaralingam, P., Sivanesan, S. and Ravikumar, L., Effective removal of heavy metal ions from aqueous solutions using a new chelating resin poly[2,5-(1,3,4-thiadiazole)-benzalimine]: Kinetic and thermodynamic study, J. *Wat. Reuse Desal.*, 6(2), 310-324(2015). https://doi.org/10.2166/wrd.2015.013).

Langmuir, I., The adsorption of gases on plane surfaces of glass, mica and platinum, *J. Am. Chem. Soc*., 40(9), 1361–1403(1918). https://doi.org/10.1021/ja02242a004

Liang, Z., Wang, Y. X., Zhou, Y. and Liu, H., Coagulation removal of melanoidins from biologically treated molasses wastewater using ferric chloride, *Chem. Eng. J.*, 152(1), 88–94(2009). https://doi.org/10.1016/j.cej.2009.03.036

Liu, J., Shao, M., Li, Q., Wu, J., Xie, B., Zhang, S. and Qian, Y., Benzene-thermal route to carbon nanotubes at a moderate temperature, *Carbon*, 40, 2961-2973(2000).

Mahmoodian, H., Moradi, O., Shariatzadeha, B., Saleh, T. A., Tyagi, I., Maity, A., Asif, M. and Gupta, V. K., Enhanced removal of methyl orange from aqueous solutions by poly HEMA-Chitosan-MWCNT nano-composite, *J. Mol. Liq.*, 202, 189–198(2014). https://doi.org/10.1016/j.molliq.2014.10.040

Marti, N., Bouzas, A., Seco, A. and Ferrer, J., Struvite precipitation assessment in anaerobic digestion processes, *Chem. Eng. J*., 141 (1), 67–74(2008). https://doi.org/10.1016/j.cej.2007.10.023

Murugesan, A., Vidhyadevi, T., Kalaivani, S. S., Premkumar, M. P., Ravikumar, L. and Sivanesan, S., Kinetic and thermodynamic studies on the removal of Zn2+ and Ni 2i+ from their aqueous solution using poly(pheylthiourea)imine, *Chem. Eng. J*. 197, 368-378(2012). https://doi.org/10.1016/j.cej.2012.05.027

Nekouei, F., Nekouei, S., Tyagi, I. and Gupta, V. K., Kinetic, thermodynamic and isotherm studies for acid blue 129 removal from liquids using copper oxide nanoparticle-modified activated carbon as a novel adsorbent, J. Mol. Liq. 201, 124–133(2015). https://doi.org/10.1016/j.molliq.2014.09.027

Nyamori, V. O., Mhlanga, S. D. and Coville, N. J., The use of organometallic transition metal complexes in the synthesis of shaped carbon nanomaterials, J. Organomet. Chem., 693(13), 2205-2222(2008). https://doi.org/10.1016/j.jorganchem.2008.04.003

Rafique, M. M. A. and Iqbal, J., Production of caron nanotubes by different routes-A review, *J. Encapsulation Adsorption. Sci*., 1 (2), 29-34(2011). https://doi.org/10.4236/jeas.2011.12004

Redlich, O. and Peterson, D. L., A useful Adsorption isotherm, *J. Phys. Chem*., 63(6), 1024-1026(1959). https://doi.org/10.1021/j150576a611

Roberts, J. D. and Caserio, M. C., Basic Principles of Organic Chemistry, 2nd ed. W.A. Benjamin Incorporation, London, 1977.

Sadegh, H., Shahryari-Ghoshekandi, R., Agarwal, S., Tyagi, I., Asif, M. and Gupta, V. K., Microwave-assisted removal of malachite green by carboxylate functionalized multi-walled carbon nanotubes: Kinetics and equilibrium study, *J. Mol. Liq*., 206, 151–158(2015b). https://doi.org/10.1016/j.molliq.2015.02.007

Sadegh, H., Shahryari-Ghoshekandi, R., Tyagi, I., Agarwal, S. and Gupta, V. K., Kinetic and thermodynamic studies for alizarin removal from liquid phase using poly-2-hydroxyethyl methacrylate (PHEMA), *J. Mol. Liq*., 207, 21–27(2015a). https://doi.org/10.1016/j.molliq.2015.03.014

Shahryari-Ghoshekandi, R. and Sadegh, H., Kinetic study of the adsorption of synthetic dyes on graphene surfaces, *Jordan J. Chem*., 9 (4), 267–278(2014).

Shooto, D. N. and Dikio, E. D., Morphological characterization of Soot from the combustion of candle wax, *Int. J. Electrochem. Sci*., 6, 1269 – 1276(2011).

Temkin, M. J. and Pyzhev, V., Recent modifications to Langmuir isotherms, *Acta Physicochim. URSS*, 12, 217–225(1940).

Sips, R., On the structure of a catalyst surface, *J. Chem. Phys.*, 16, 490–495(1948). https://doi.org/10.1063/1.1746922

Terrones, M., Science and Technology of the twenty-first century: Synthesis, properties and applications of carbon nanotubes, *Annu. Rev. Mater. Res*., 33 (1) 419–501(2003). https://doi.org/10.1146/annurev.matsci.33.012802.100255

Toth, J., State equations of the solid-gas interface layer, *Acta Chim. Acad. Sci. Hung*., 69, 311-317(1971).

Vidhyadevi, T., Murugesan, A., Kirupha, A. D., Baskaralingam, P., Ravikumar, L. and Sivanesan, S., Adsorption of Congo Red dye over pendent chlorobenzylidine rings present on polythioamide resin: Kinetic and equilibrium studies, *Separ. Sci. Technol.*, 48(10), 1450-1458(2013). https://doi.org/10.1080/01496395.2012.726306

Vijayaraghavan, K., Padmesh, T. V., Palanivelu, K. and Velan, M., Biosorption of nickel (II) ions onto sargassum wightii: Application of two-parameter and three-parameter isotherm models, *J. Hazard. Mater. B.*, 133(1-3), 304 –308(2006). https://doi.org/10.1016/j.jhazmat.2005.10.016

Wang, X., Lu, J. and Xing, B. S., Sorption of organic contaminants by carbon nanotubes: Influence of adsorbed organic matter, *Environ. Sci. Technol*. 42 (9), 3207–3212(2008). https://doi.org/10.1021/es702971g

Zare, K., Sadegh, H., Shahryari-Ghoshekandi, R., Maazinejad, B., Ali, V., Tyagi, I., Agarwal, S. and Gupta, V. K., *J. Mol. Liq.*, 212, 266-271(2015).